International Journal of Neural Systems

ROBUST WAVELET STABILIZED 'FOOTPRINTS OF UNCERTAINTY' FOR FUZZY SYSTEM CLASSIFIERS TO AUTOMATICALLY DETECT SHARP WAVES IN THE EEG AFTER HYPOXIA ISCHEMIA

HAMID ABBASI
Department of Engineering Science, The University of Auckland
Auckland, New Zealand
h.abbasi@auckland.ac.nz

LAURA BENNET
Department of Physiology, Faculty of Medical and Health Sciences
The University of Auckland
Auckland, New Zealand
l.bennet@auckland.ac.nz

ALISTAIR J. GUNN
Department of Physiology, Faculty of Medical and Health Sciences
The University of Auckland
Auckland, New Zealand
aj.gunn@auckland.ac.nz

CHARLES P. UNSWORTH*
Department of Engineering Science, The University of Auckland
Auckland, New Zealand
c.unsworth@auckland.ac.nz

Currently, there are no developed methods to detect sharp wave transients that exist in the latent phase after hypoxia-ischemia (HI) in the Electroencephalogram (EEG) in order to determine if these micro-scale transients are potential biomarkers of HI. A major issue with sharp waves in the HI-EEG is that they possess a large variability in their sharp wave profile making it difficult to build a compact 'Footprint of Uncertainty' (FOU) required for ideal performance of a Type-2 Fuzzy logic system (FLS) classifier. In this article, we develop a novel computational EEG analysis method to robustly detect sharp waves using over 30 hours of post occlusion HI-EEG from an equivalent, in utero, preterm fetal sheep model cohort. We demonstrate that initial wavelet transform (WT) of the sharp waves stabilizes the variation in their profile and thus permits a highly compact FOU to be built, hence, optimizing the performance of a Type-2 FLS. We demonstrate that this method leads to higher overall performance of 94%±1 for the clinical 64Hz sampled EEG and 97%±1 for the high resolution 1024Hz sampled EEG that is improved upon over conventional standard wavelet 67%±5 and 82%±3 respectively and fuzzy approaches 88%±2 and 90%±3 respectively when performed in isolation.

Keywords: EEG, Hypoxic-Ischemic Encephalopathy (HIE), High frequency micro-scale seizures, sharp wave detection, Type-2 Fuzzy, Wavelet transform, Machine learning, Automatic detection

* Corresponding author.

International Journal of Neural Systems

1. Introduction

Hypoxia-ischemia (HI) at birth can lead to acute HI encephalopathy (HIE) and ultimately to brain injury. The risk of injury is much higher in babies born preterm [1-3]. Importantly, injury evolves over time, and many brain cells die over hours to days after an HI insult [3, 4]. This delay in injury offers a window of opportunity for neuroprotective treatments. Pre-clinical animal studies in term fetuses and neonates have shown that after a severe HI insult, there is restoration of oxidative metabolism in a 'latent' phase lasting around 6 hours. This is followed by a secondary loss of oxidative metabolism lasting around 48-72 hours, during which time most brain cells die [2, 4]. The timing of these phases is broadly similar for the preterm brain [5, 6]. Cerebral hypothermia is now used clinically for term infants with evidence of moderate to severe HIE [2, 4, 7], but animal studies show that it is only effective if started during the latent phase of recovery [2, 4]. Clinically, despite starting cooling early after birth, only one baby in every 6-8 benefits from hypothermia [7]. This, largely, reflects the fact that many babies are born with brain injury which has evolved beyond the latent phase [6]. However, currently, we do not have reliable biomarkers which can allow us to determine the phase of injury and thus which babies will benefit from treatment [6]. Such biomarkers would also help refine the use of hypothermia for term infants, and for the development of new neuroprotection therapies for term and preterm babies.

Electroencephalographic (EEG) monitoring is increasingly used to assess the neurological well-being of newborn infants [3]. Two lead amplitude-integrated EEG (aEEG) recordings are most commonly used to assess newborn EEG. Although aEEG readily identifies large amplitude seizures it does not readily allow for detection of more subtle low amplitude high frequency events [3] which our preclinical animal studies have shown are important [3, 6]. A number of other pre-clinical and clinical studies have been conducted on existence of HI transients along the EEG which have shown a correlation between events and outcomes [8-10]. Our pre-clinical observations in preterm fetal sheep after asphyxia, using raw signals from two lead EEG recordings, have shown that high frequency epileptiform transients (spikes, sharps and slow-waves) [5, 11, 12] occur primarily in the latent phase peaking around 2-3 hours after the end of HI [5, 13, 14] and that numbers of latent phase transients correlate with neurological outcome [5, 6]. Thus, transient identification and quantification in the latent phase of injury may provide useful biomarkers for identifying and assessing preterm infants who have been exposed to HI (Figure 1). The present study addresses ways of automatic detection of sharp wave epileptiform transients in the EEG after HI. In contrast, the majority of research to date has focussed on automatic diagnosis of neurological disorders [15] as well as automatic detection of spike waves for seizure detection, in the epileptic EEG, summarized in papers involving prediction with linear and nonlinear methods [16], wavelet methods [17, 18], spike sorting techniques [19], kernel methods [20, 21] and neural network prediction [22-24] with some cot side systems being available [25]. HI induced seizures have been studied in several animal models, reviewed in [26] with morphological operators being used to improve automated spike wave detection in seizures [27] and unsupervised methods [28] from the HI EEG of the neonatal rat. We have previously reported the utility of short-time Fourier (STFT), Haar and Reverse Bi-orthogonal wavelet transform (WT) and Type-2 fuzzy logic system (FLS) classifiers for spike transient identification [11, 12, 29, 30] in the EEG sampled at 64Hz from preterm fetal sheep.

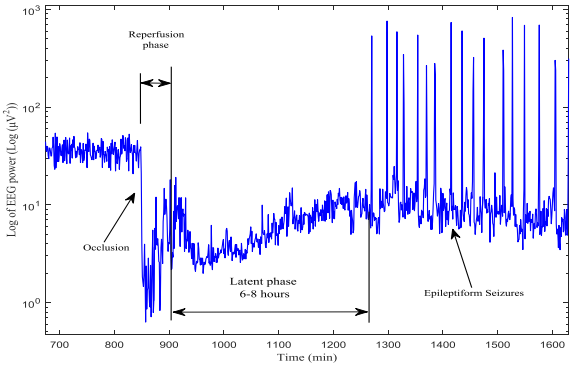

Fig. 1. The latent phase of injury after a hypoxic insult.

Automated detection methods since 2011 have been reported to improve the accuracy of seizure detection in the HI EEG of human neonates [31]. These studies have demonstrated that quantitative EEG (qEEG) measures such as relative delta power, skewness, kurtosis, amplitude, and discontinuity can be used to separate between HIE grades. A neonatal HI EEG research group, Temko et.al, have applied support vector machines (SVMs) to discriminate between seizure and non-seizure EEG epochs [32, 33], and probabilistic modelling to improve the prediction of seizures in the EEG of neonates exposed to HI [34, 35].

By contrast, our work differs by being concerned in the identification of HI sharp wave epileptiform transients in the latent phase of the EEG, before high amplitude seizures occur. There is no current method for the accurate identification and quantification of sharp wave transients in the EEG after HI. Fetal sheep EEG data are often collected at a relatively low sampling rate of 64Hz, which could also limit the accurate detection and quantification of transients [5, 11, 12, 29]. This is in comparison to human models which use the clinical sample rates of 64Hz have been employed in [36, 37] and recently higher sample rates of 256Hz employed in [32, 33]. We have recently presented preliminary results of how the WT-Type-2-FLS method can detect sharp wave transients at a conference [38]. This paper presents, for the first time, a WT-Type-2-FLS method to accurately detect and quantify epileptiform sharp wave transients in the EEG recorded after HI and determines a suitable wavelet for both typical clinical 64Hz sampling of the EEG and high, research-based sampling at 1024Hz.

Current work is performed using over 30 hours of data collected after HI induced by a period of umbilical cord occlusion from a cohort of preterm-equivalent, anaesthetized fetal sheep, studied *in utero*. This provided more than 5000 individual sharp waves for analysis, which is larger than studied in most previous studies [39]. We demonstrate that a significant performance gain can be achieved using the developed WT-Type-2-FLS method over standalone wavelet or fuzzy methods.

2. Data Acquisition

2.1. *Experimental procedures*

All the animal procedures for acquisition of the data sets were approved by the Animal Ethics Committee of the University of Auckland and in accordance with the Animal Welfare Act (1999) of New Zealand. Data used in this study were obtained from preterm fetal sheep at 0.7 gestation (equivalent to a 27-30 week human in terms of brain maturation) [40]. Under general anesthesia and using aseptic techniques, five fetal sheep were instrumented with catheters and electrodes as previously described [5, 13]. For the purposes of this study, 4 EEG electrodes (two on the left side of the head, two on the right side of the head), plus a ground electrode were used in the measurement of fetal EEG (made in-house from AS633-5SSF wire; Cooner Wire, Chatsworth, CA, USA). These electrodes were placed through burr holes onto the dura over the parasagittal parietal cortex (5 and 10 mm anterior to bregma and 5 mm lateral). A standard montage was not used rather one electrode was used to measure the potential difference relative to the second electrode on the left side of the head, and similarly this was performed for the two electrodes on the right side of the head. The data sets used in the study were drawn from the differential set of electrodes on the left side of the head. Burr holes were filled with surgical bone wax and the electrodes secured with cyanoacrylate glue. A reference electrode was sewn over the occiput. We use EEG recorded from the extradural space because the fetus is highly active and suspended in an electrolyte solution similar to plasma, that is to say, the amniotic fluid. In this unique environment extradural recordings provide a far superior signal to surface recordings with minimal movement artifact. We anticipate that higher-frequencies recorded on the extradural surface may have greater resolution than surface EEG, as suggested by [41]. These issues are much less important in the postnatal environment where preterm infants are not able to move much. A silicone occluder was placed around the umbilical cord, for later inflation to produce HI. Fetuses were returned to the uterus, and ewes and their fetuses were allowed five days to recovery from surgery and anesthesia before experiments began. Fetuses were studied at 103.4±0.6 days (term =147 days). On the day of experiment fetal HI was induced by complete occlusion of the umbilical cord for 25 minutes [5, 13]. The occluder was then released, fetuses returned to normoxic conditions, and the fetal EEG was studied during the first 6 hours of recovery (the latent phase).

2.2. *Data collection*

EEG data were continuously recorded through two channels using Labview (Labview for Windows, National Instruments, TX, USA) and digitized at a sampling frequency of 1024 Hz. For reliable high resolution EEG sampling, EEG signals were recorded via leads through a head-stage with an overall gain of 10,000 which aided primary noise reduction of the signal. Analogue signals were then processed with a 6th order low-pass Butterworth anti-aliasing filter, with cutoff frequency of 512 Hz and a high-pass filter of 1.6 Hz. EEG signals were saved at 1024 Hz. Since the study was conducted in utero there was no need to have an additional notch filter to filter out 50Hz. The recorded data were then decoded and extracted into Matlab for analysis. In order to compare the performance of the WT-Type-2-FLS to typical sampling rates in fetal sheep

studies, the data was then down sampled to 64Hz digitally with a second anti-aliasing filter with cutoff frequency of 32Hz. The data sets were zero-meaned and noise removed using a finite impulse response (FIR) band-pass digital filter of order 100 with a stop-band frequency range of $0.05 \leq \omega \leq 0.13$. A sample section of the EEG from the latent phase of recovery containing HI spikes, sharp waves, slow waves and compounds of these transients (known as complexes) are shown in figure 2(A). HI sharp wave transients in the fetal sheep model differ slightly from the conventional sharp wave definition in conventional human EEG [42]. HI sharp wave transients in the fetal sheep models have been defined in general to have amplitude >10μV and a duration between 70 and 250ms [43]. However, the amplitude of HI sharp wave transients in the fetal sheep model has been known to vary, being observed to be >25μV in the early latent phase [44] and >50μV under maternal dexamethasone [45]. From the definitions stated above and from our preliminary investigations [38] we found that an amplitude of 20μV served to suppress noise and identify the most number of sharp waves that occur in HI EEG of the fetal sheep model. Hence, the HI sharp wave transients in the fetal sheep model in both data sets were identified manually by an expert to these criteria. In addition, sharp wave transients that existed in complexes were also identified by the expert in order to enable more robust FOUs to be built to detect sharp waves that appeared in more complicated regions of the data.

Table 1, highlights the total number of sharp waves identified by an expert (namely sum of the correct detections and the missed patterns by the algorithm) in the whole of the latent phase of each sheep used in the study.

Figure 2(A) highlights a typical section of post-HI EEG that contains typical spike, sharp wave, slow wave and complex wave transients. Figure 2(B-C) shows the sharp wave profiles in the EEG of all the sheep for 1024Hz and 64Hz, respectively. Note that the sharp waveforms in figures 2(B-C) have considerable variance. From this we postulated that using only a wavelet transform may lead to a poor sharp wave detection performance. In addition, the large variance of the sharp waveforms would rule out the use of a Type-1-FLS classifier. While a Type-2-FLS classifier would be the most appropriate choice we postulated that the large FOU space built to envelope the sharp waves would also result in a poor performance for detection if a Type-2 fuzzy system was used in isolation.

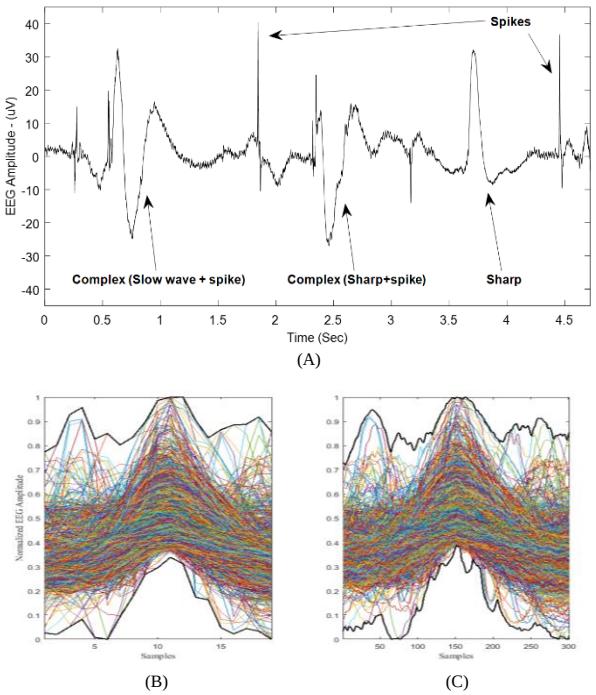

Fig. 2. (A) Sample Spikes and Sharp waves during the latent phase of recovery after HI EEG, (B) Sharp profiles from 5 sheep at 64Hz sampling, (C) Sharp profiles from 5 sheep at 1024Hz sampling.

Table 1. The total number of identified sharp waves by an expert along the entire latent phase of each sheep.

Animal number	1	2	3	4	5
Sharps waves	449	243	598	1062	2834

In this paper, we demonstrate how the initial application of a suitably chosen wavelet transform can be used to stabilize the transformed sharp wave profiles considerably. This then allows for a robust FOU to be built that can be subsequently passed to a Type-2-FLS classifier resulting in high performance in comparison to the direct application of wavelet and fuzzy methods separately to the original sharp waves in post-HI EEG recordings.

3. Methods

In this section, we introduce wavelet transform (WT) methods and fuzzy logic system (FLS) classifiers. This is followed by an overview of our developed WT- Type-2 FLS classifier and the feature extraction necessary to provide reliable identification of sharp waves in high and low frequency sampled post-HI EEG signals.

3.1. *The Wavelet Transform*

The Wavelet Transform (WT) is a flexible time-frequency multi-resolution technique that can decompose a signal into different frequency scales [46, 47]. Wavelet techniques have broad application in medical and biomedical fields such as monitoring fetal and adult heart rate variability, ECG feature extraction and diagnostic assessment and frequency decomposition of ultrasound images [47-49]. They have been extensively applied to analysis of epileptiform activity [17], brain MRI [50], diagnosis of ADHD [51], Alzheimer's diseases [52-55] and autistic spectrum disorder [56]. Although, some recent works, based on the metaheuristics and enhanced probabilistic neural network, have shown enhancements for combination of classifiers and cluster ensembles [57-60], but wavelet techniques are highly useful for many facets of signal processing, such as: edge detection, approximation, compression, de-noising and classification [61]. The Continuous Wavelet Transform (CWT) of a signal $s(t)$ is defined as

$$CWT(a,b) = \frac{1}{\sqrt{a}}\int_{-\infty}^{\infty} s(t)\varphi^*\left(\frac{t-b}{a}\right)dt \qquad (1)$$

Where $\varphi(t)$ represents a basis function known as the 'Mother wavelet', '*' denotes complex conjugate, and a, b are the dilation and translation factors of the mother wavelet [61, 62]. The two key properties of wavelets are 'dilation' where the mother wavelet becomes "stretched" to different scales and "translation" where the scaled wavelet is shifted in time. It is the "dilating and translating" of a chosen mother wavelet that allows one to correlate it with similar hidden events in a signal. This discloses the frequency and location of the desired event in time and helps one to detect specific shape profiles.

3.2. *Justifying an appropriate wavelet basis*

Initial determination of an appropriate wavelet family was made by visually inspecting the similarity that a wavelet had to a sharp wave. On observation of a typical sharp profile, Daubechies and Gaussian wavelet families intuitively came to mind. We then narrowed this choice down further, by determining which wavelet in the family provided the highest cross-correlation [63] and the lowest minimum Shannon entropy [61] to the sharp wave at both 64Hz and 1024Hz sampling rates. For completeness, this was performed on the Daubechies and Gaussian wavelet families [64] for the wavelets with vanishing moments 1-3 with software written in Matlab. The normalised cross-correlation was determined for every sharp wave profile against each individual wavelet in the Daubechies and Gaussian wavelet families, for vanishing moments 1-3. The 'average normalized cross-correlation', figure 3(A) was then determined for each individual wavelet in the Daubechies and Gaussian wavelet families, for vanishing moments 1-3 from all the normalized cross-correlations of every sharp wave profile. The Minimum Shannon entropy criterion [61], S, was also used to assess how similar the wavelets in the Daubechies and Gaussian wavelet families, figure 3(B), for vanishing moments 1-3 were to the sharp waves.

As one can observe from Figure 3(A) and figure 3(B) both the Gaussian 2 and Daubechies 2 wavelet provided the highest cross-correlations and minimum Shannon entropies for both the 1024Hz and 64Hz versions of the sharp wave signals. It was found that scale 15 of Daubechies 2 corresponded to the temporal length of the 64Hz sharp waves and scale 32 corresponded to the temporal length of the 1024Hz sharp waves. Thus, we would *hypothesis* that Gaussian 2 and Daubechies 2 wavelets would be reasonable and logical choice for sharp wave detection. This is also in agreement with the 'general rule of thumb'- that the number of vanishing moments of the wavelet should tally with the same number of vanishing moments as a sharp wave respectively (namely, 2). In section 4.1, we initially assess how the Gaussian 2, scale 32 and Daubechies 2, scale 15 wavelets perform (i.e. a wavelet-only approach) when directly applied at different magnitude threshold values (0-4-0.7) in the 64Hz and 1024Hz sampled HI EEG.

3.3. *Fuzzy Inference Systems*

Fuzzy logic systems (FLS) [65] provide a framework to embed human observed priories via a set of logic rule-bases [65] known as Type-1 and Type-2 Fuzzy Logic Systems (FLS) [65, 66]. FLSs have been used in biomedical classification of epileptic seizure and spike sorting applications [29, 67-71] as well as diagnosis of autism spectrum disorder and ADHD [72, 73]. Fuzzy Logic Systems (FLS) [47, 74, 75] are structured on a set of primary IF-THEN logical rules which are used to embed the knowledge of an expert into the FLS's Membership Functions (MFs). In such a system, each rule maps multiple inputs from input MFs to one or more outputs on output MFs. Type-1 FLS are very specific and do not accommodate variance of the signal of interest well, which is a common

problem in real-world data and when noise is present. The Type-2 FLS overcomes the issues encountered in Type-1 FLS by employing a Footprint of Uncertainty (FOU), namely a region which accounts for the variance that exists in the signal of interest [65, 66]. In this study, the FOU consists of all the MFs that represent a collection of sharp waves identified by an expert. Thus, a typical format of a Type-2 fuzzy Multi Input Single Output (MISO) rule for a Type-2 fuzzy classifier for the detection of sharp waves is represented as:

$$\begin{aligned} &If\ f(LMF) \le f\big(W(signal)\big) \le f(UMF), \\ &\quad Then \quad Class\ is\ \text{'Sharp wave detected'} \\ &\quad Else \quad Class\ is\ \text{'Not Sharp wave'} \end{aligned} \tag{2}$$

Where, LMF and UMF are the lower and upper Type-2 input MFs, respectively [76]. Several Type-2 Fuzzy rules are then defined by an expert in the rule-base of the purposed Type-2 FLS classifier. In this study, these rules are executed, known as 'firing, on the wavelet decomposition of the post-HI EEG and the output of the Type-2 FLS classifier identifies whether a detection of a sharp-wave has occurred.

3.4. *The WT-Type-2-Fuzzy classifier*

In this article, we *hypothesize* that the wavelet transform of the raw sharp waves will provide a more robust FOU than a FOU based directly on the raw sharp wave profiles themselves, hence, significantly improving the performance of Fuzzy Type-2 classifier. As will be discussed later in section 4.2, the FOUs built from the sharp waves directly had large variance and were not robust. Thus, we *hypothesise* that stable FOUs could be obtained by performing an initial wavelet transformation using an appropriate wavelet basis and using the transformed signal to indirectly build compact FOUs. Thus, all that would be necessary would be to visually identify a suitable wavelet scale that provided a smooth compact transformation.

3.5. *Performance measures*

For the sensitivity and selectivity criteria [12], equations 3 to 5 were used to evaluate the performance of the WT-Type-2-FLS classifier, defined as:

$$Sensitivity = \frac{TP}{TP + FN} * 100 \tag{3}$$

$$Selectivity = \frac{TP}{TP + FP} * 100 \tag{4}$$

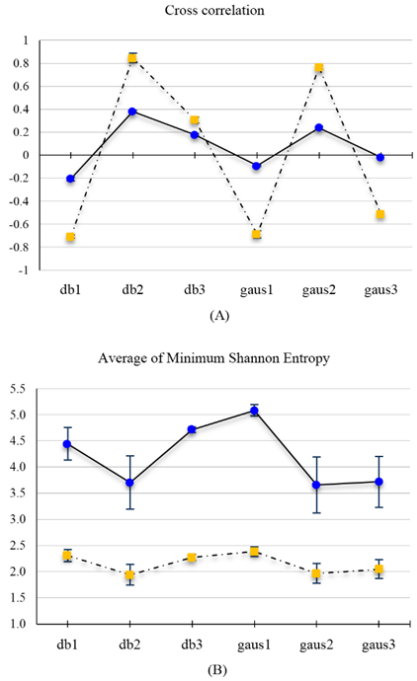

Fig. 3. (A) Cross correlation results for both the Gaussian and Daubechies wavelet families at 64Hz (dotted lines-orange squares) and 1024Hz (solid lines-blue circles); (B) Average Minimum Shannon Entropy for both the Gaussian and Daubechies and wavelet families at 64Hz (dotted lines-orange squares) and 1024Hz (solid lines-blue circles).

$$Overall\ performance = \frac{(Sensitivity + Selectivity)}{2} \tag{5}$$

A true positive (TP) is defined as a transient that is detected by both the algorithm and an expert. A false positive (FP) detection occurs when the algorithm detects another transient which is not a sharp wave and not specified by an expert. Finally a sharp wave that is identified by an expert but not detected by the algorithm is deemed to be a false negative (FN).

4. Results

In this section, we present performance results for the detection of sharp waves in the post-HI EEG of the preterm fetal sheep using the following methods:

(i) Conventional Wavelet Performance – performance of Gaussian 2, scale 32 and Daubechies 2, scale 15 wavelets applied directly to the post-HI EEG of the fetal sheep for varying magnitude threshold values (detailed in section 4.1).

(ii) Conventional Type-2 Fuzzy Performance – performance of Type-2-Fuzzy classifier applied to FOUs built directly from the raw sharp waves themselves of the post-HI EEG of the fetal sheep (detailed in section 4.2).

(iii)Performance of the developed WT- Type-2-Fuzzy classifier where the FOUs are indirectly built up from the wavelet transformations of the sharp waves of the post-HI EEG of the fetal sheep (detailed in section 4.3).

4.1. *Conventional Wavelet Performance*

We initially assessed how the Gaussian 2, scale 32 and Daubechies 2, scale 15 wavelets performed when directly applied at different magnitude threshold values in the 64Hz and 1024Hz sampled HI EEG. Results from the wavelet-only approach are presented in figure 4.

Figure 4 shows the average overall performance, using the recordings from all 5 sheep, of the wavelet-only approach for different threshold levels for the Daubechies 2, scale 15 wavelet applied to the 64Hz EEG (dotted line-red squares) and the Gaussian 2, scale 32 wavelet applied to the 1024Hz EEG (solid line-blue circles). It can be seen that the average overall performance increases to a maximum of 67.4%±4.7 for the Daubechies 2, scale 15 wavelet of the 64Hz EEG and 82.1%±3.0 for the Gaussian 2, scale 32 wavelet of the 1024Hz EEG when the threshold value is 0.5 and decreases thereafter. Hence, the best detector of sharp waves using a standard wavelet-only approach would be the Gaussian 2, scale 32 wavelet when used on a 1024Hz sampled EEG. It was found that higher numbers of false positives (FP) and false negatives (FN) contributed to the reduced overall performance of the wavelet-only method.

4.2. *Conventional Type-2 Fuzzy Performance*

FOUs were constructed directly from sharp waves by defining an envelope around the mean to build an FOU, for all the different combinations of the sheep cohort, shown in Figure 5(A) for the 64Hz sampled EEG, and Figure 5(B) for the 1024Hz sampled EEG.

FOUs constructed directly from the sharp waves did not provide stable and consistent FOUs, as shown in figure 5(A-B), which should lead to a low performance of the Type-2-FLS classifier due to large variance in the FOU. Figure 10(A), highlights the low performance expected of the Type-2-FLS using the FOU's defined using 1,2,3 and 4 sheep (where the method of building a robust FOU is described in detail in section 4.4) due to the large variance FOU's of Figure 5(A-B).

4.3. *The Developed WT-Type-2-Fuzzy Performance*

Smooth compact transformations were observed for the Gaussian 2 wavelet at scale 3 for the 64Hz sampled post-HI EEG, figure 6(B) and at scale 32 for the 1024Hz sampled post-HI EEG, figure 6(H). For the Daubechies 2 wavelet, smooth compact transformations were observed at scale 3 in the 64Hz sampled post-HI EEG, figure 7(C), however, no smooth compact support was observed for the 1024Hz sampled post-HI EEG, figure 7(F-H).

FOUs were then built from wavelet transformations of the sharp waves for the scales that were identified as having smooth compact wavelet transformations. Figure 8 shows the FOUs obtained from the Gaussian 2 transformations for scale 3 at 64Hz and scale 32 at 1024Hz. As can be seen, the FOUs built from the wavelet transformations of the sharps, figure 8(B), are highly compact and should result in a good Type-2 FLS performance. Figure 9(A) shows the FOUs obtained from the Daubechies 2 transformation for scale 15 at 64Hz. As can be seen the FOUs built from this selected scale is also highly compact and should result in a good Type-2 FLS performance. We have also included the FOU of a highly irregular wavelet transformation, figure 9(B), which corresponds to Daubechies 2, scale 32 at 1024Hz shown in figure 7(H), to highlight how this leads to a non-stable FOU which should yield a poor classification performance. The developed WT-Type-2-Fuzzy system then took particular features from the FOUs, described above, to build a fuzzy rule-base that could be then passed to the Type-2-Fuzzy classifier. We define 2 features of the FOU: the function that defines the envelope of the upper bounds of all the wavelet transformed sharp waves, denoted as the Upper Membership Function (UMF), and the function that defines the envelope of the lower bounds of all the wavelet transformed sharp waves, denoted as the Lower Membership Function (LMF). In this manner, the wavelet transformed (W) EEG was passed to the Type-2-Fuzzy classifier and performance was measured against an experts prior identification of the sharps waves in the EEG.

4.4. *Building a robust FOU*

We next addressed the question of how many sharp waves are necessary to build a suitable FOU that was sufficiently reliable to predict the unseen sharp waves to a high degree of accuracy. In addition, one consideration of the nature of this work is the experimentally difficulty, expense and time required to obtain data from the sheep model *in utero* (described in section 2.2). Thus, obtaining an FOU from as few sheep as possible would be highly

desirable. Our approach to tackling this issue was to build separate FOU's from the whole latent phases of sheep 1, 2, 3 and 4. The constructed FOUs could then be tested out on the remaining sheep whose latent phase was not used in building the FOU's. For example, the top row of Figure 5(A) depicts the FOU's constructed from the raw sharp waves that existed in the entire latent phase for each of the 5 sheep. Thus, the FOU for sheep fetus 1 in figure 5(A) could be considered to be our training set and the prediction performance of this FOU could be estimated by essentially validating it on the average number of sharps correctly detected in the latent phases of the remaining sheep fetus's 2, 3, 4 and 5. In addition, this approach could be 'bootstrapped' [77, 78] by then using the FOU of sheep fetus 2 and validating it on the average number of sharps correctly detected in the latent phases of the remaining sheep 1, 3, 4, and 5. Furthermore, FOU's were then constructed of 2 sheep, 3 sheep and 4 sheep (as shown in figure 5, rows 2-4) and tested on the remaining sheep and permutating in a similar manner as described above for 1 sheep. The bootstrapped results from using the raw sharp wave profiles (Figure 5) as well as the wavelet transformed envelopes (Figures 8 and 9)

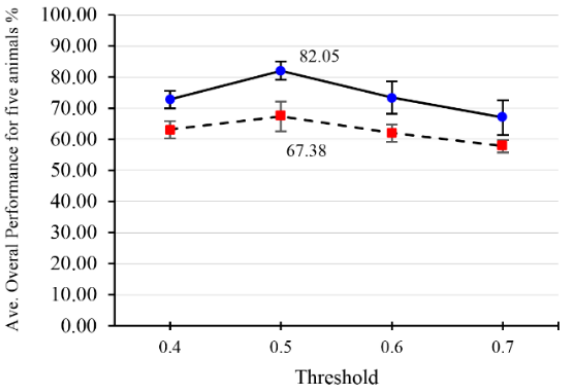

Fig. 4. The Average Overall Performance (for 5 sheep) using a standard wavelet-only approach for different threshold values. Gaussian 2, scale 32 wavelet applied to 1024Hz EEG (solid line-blue circles), Daubechies 2, scale 15 applied to 64Hz EEG (dotted line-red squares).

are given in sections 4.2 and 4.3 for the different FOUs, respectively.

5. Discussion

Figure 10(A) highlights the Type-2-FLS classifier's overall bootstrapped performance, using training sets consisting of 1-4 sheep, when passed the FOUs built from

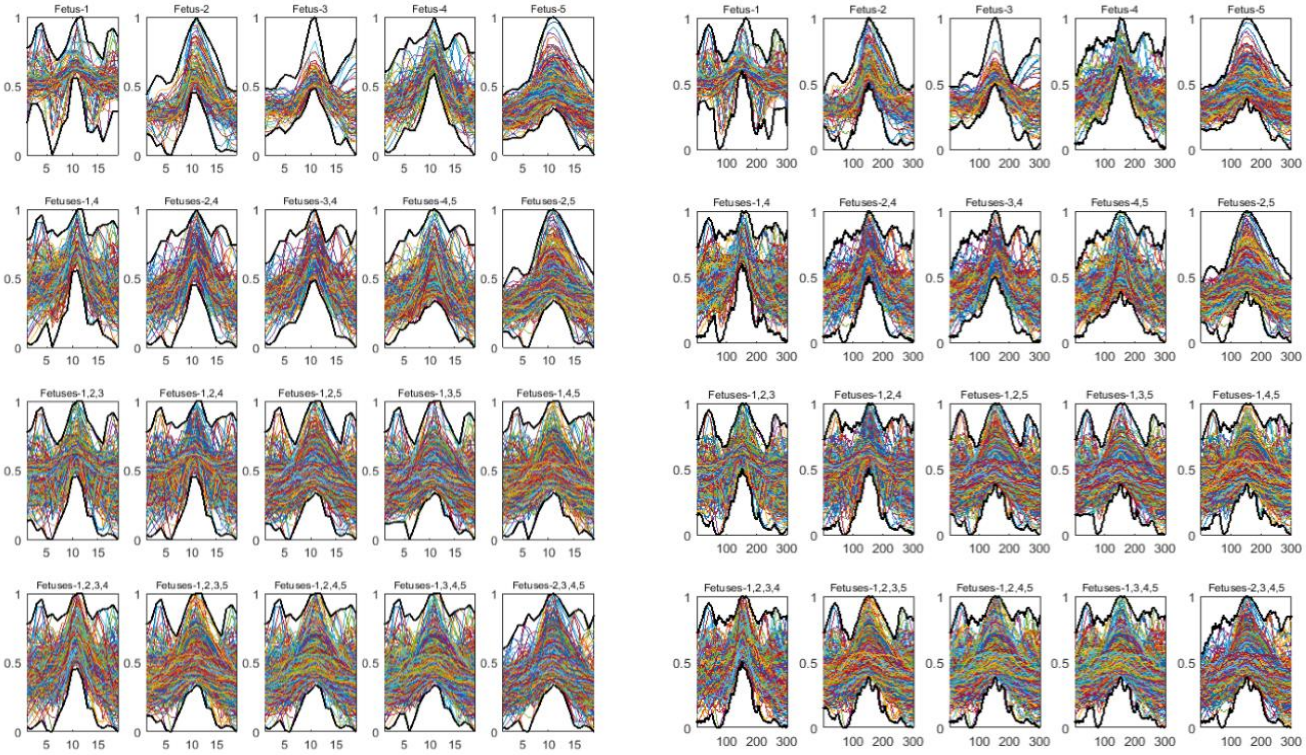

(A) (B)

Fig. 5. Typical FOUs defined for the Type-2-FLS using all the raw sharp waves for all the different combinations of the sheep cohort for: (A) 64Hz sampled EEG, (B) 1024Hz sampled EEG.

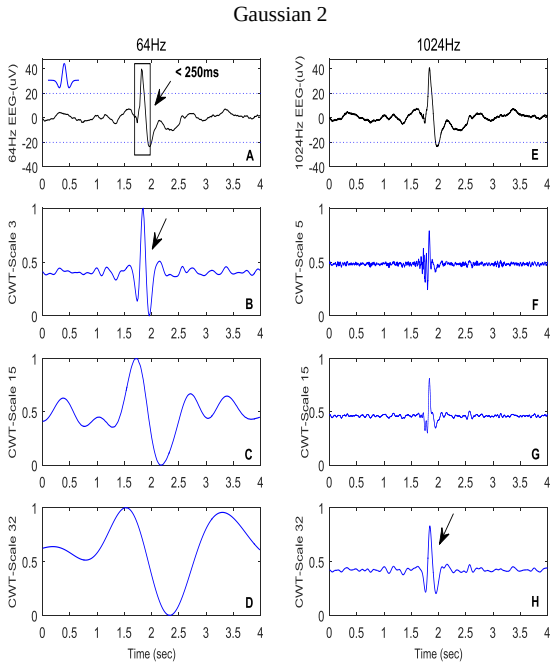

Fig. 6. (A) A sharp wave sampled at 64 Hz; Normalized Gaussian 2 wavelet coefficients of scale 3 (B), 15 (C) and 32 (D) of the 64Hz sampled sharp wave; (E) A sharp wave sampled at 1024 Hz; Normalized Gaussian 2 wavelet coefficients of scale 3 (F), 15 (G) and 32 (H) of the 64Hz sampled sharp wave.

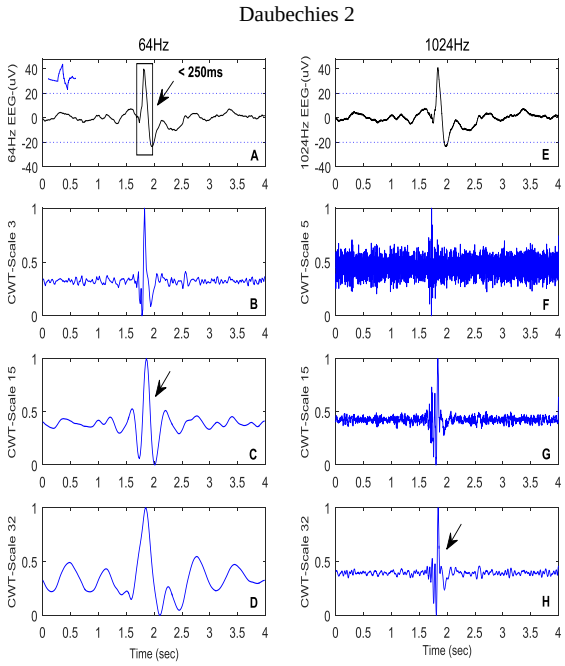

Fig. 7. (A) A sharp wave sampled at 64 Hz; Normalized Daubechies 2 wavelet coefficients of scale 3 (B), 15 (C) and 32 (D) of the 64Hz sampled sharp wave; (E) A sharp wave sampled at 1024 Hz; Normalized Daubechies 2 wavelet coefficients of scale 3 (F), 15 (G) and 32 (H) of the 1024Hz sampled sharp wave.

the raw sharp waves themselves (where the dotted line represents the 64Hz sampled EEG and the solid line the 1024Hz EEG). Similarly, Figure 10(B) highlights how the Type-2-FLS overall bootstrapped performance, using training sets consisting of 1-4 sheep, when passed the FOUs built from the wavelet transformed sharp waves (where the dotted lines again represents the 64Hz sampled EEG and the solid lines the 1024Hz EEG). It can be seen that the Type-2-FLS classifier performance improved in all cases as the FOUs were built by increasing the sheep cohort to 4.

The best performing Type-2-FLS classifier occurred when the FOUs were built from Gaussian 2, scale 32 wavelet transformations of the sharps waves for a 1024Hz sampled EEG. This provided an excellent overall performance of 97%±1, as shown in Figure 10(B). This was followed by a Type-2-FLS classifier, where the FOUs were built from Daubechies 2, scale 15, wavelet transformations of the sharp waves for a 64Hz sampled EEG, with an overall performance of 94%±1, Figure 10(B). It should be noted that both these Type-2-FLS classifiers were the ones identified as having the most stable compact wavelet transformed FOU in Figures 8(B) and 9(A) respectively. The third performing Type-2-FLS classifier used FOUs built from Gaussian 2, scale 3, wavelet transformations of the sharp waves for a 64Hz sampled EEG, with an overall performance of 93%±1, Figure 10(B). The fourth and fifth performing Type-2-FLS classifiers, were the ones where the FOUs were built from raw sharps waves for the 1024Hz and 64Hz sampled EEGs, with overall performance of 90%±3 and 88%±2, respectively, Figure 10(A). The sixth performing Type-2-FLS classifier involved FOUs built from Daubechies 2, scale 32, wavelet transformations of the sharp waves from the 1024Hz sampled EEG, with an overall performance of 83%±2, Figure 10(B). As mentioned in 4.3, this corresponded to a highly irregular, non-stable FOU that should yield a poor classification performance.

For standard equivalent wavelet-only detection, described in Section 4.1 - Figure 4, the performance was found to be 67%±5 for the Daubechies 2, scale 15 wavelet for the 64Hz EEG compared to the 94%±1 for a WT-Type-2-FLS classifier, where the FOUs were built from Daubechies 2, scale 15, wavelet transformations of the sharps waves for the 64Hz sampled EEG. Similarly, for wavelet-only detection, the performance was found to be 82%±3 for the Gaussian 2, scale 32 wavelet of the

Gaussian 2 Wavelet FOUs

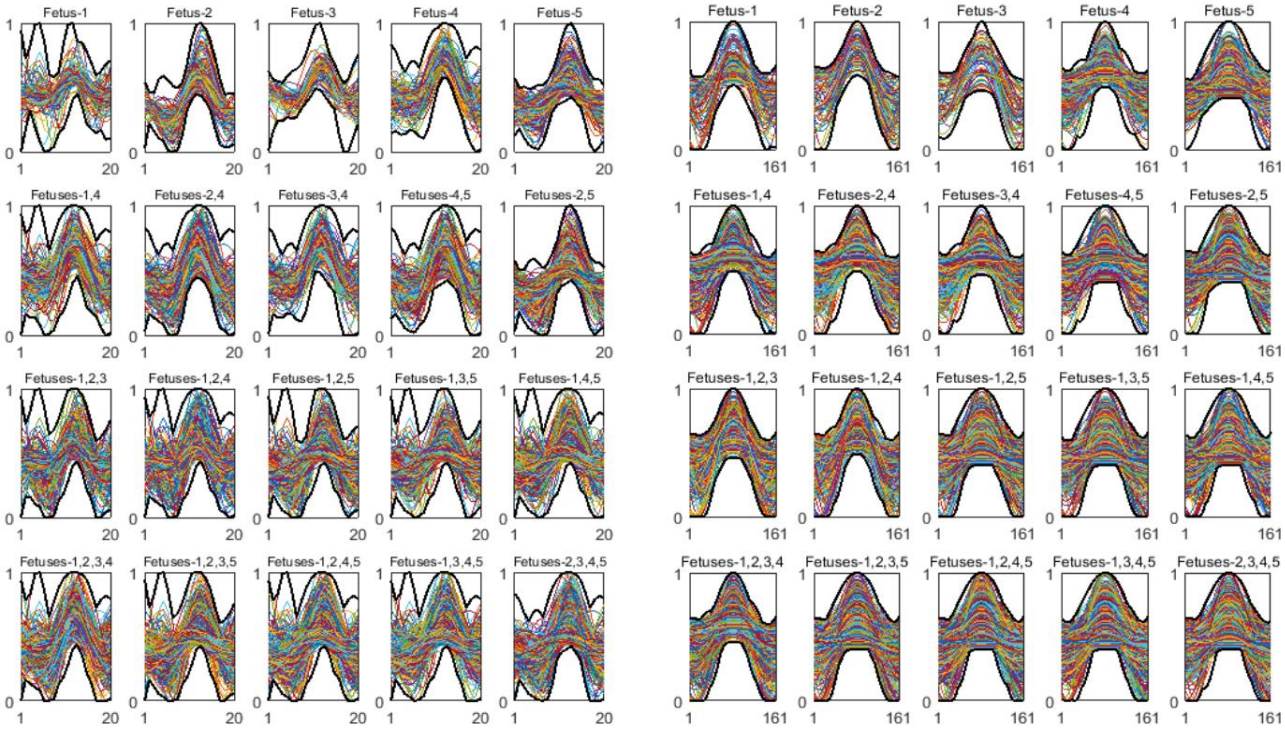

Fig. 8. FOUs obtained from: (A) Gaussian 2, scale 3 at 64Hz and (B) the Gaussian 2, scale 32 at 1024Hz

Daubechies 2 Wavelet FOUs

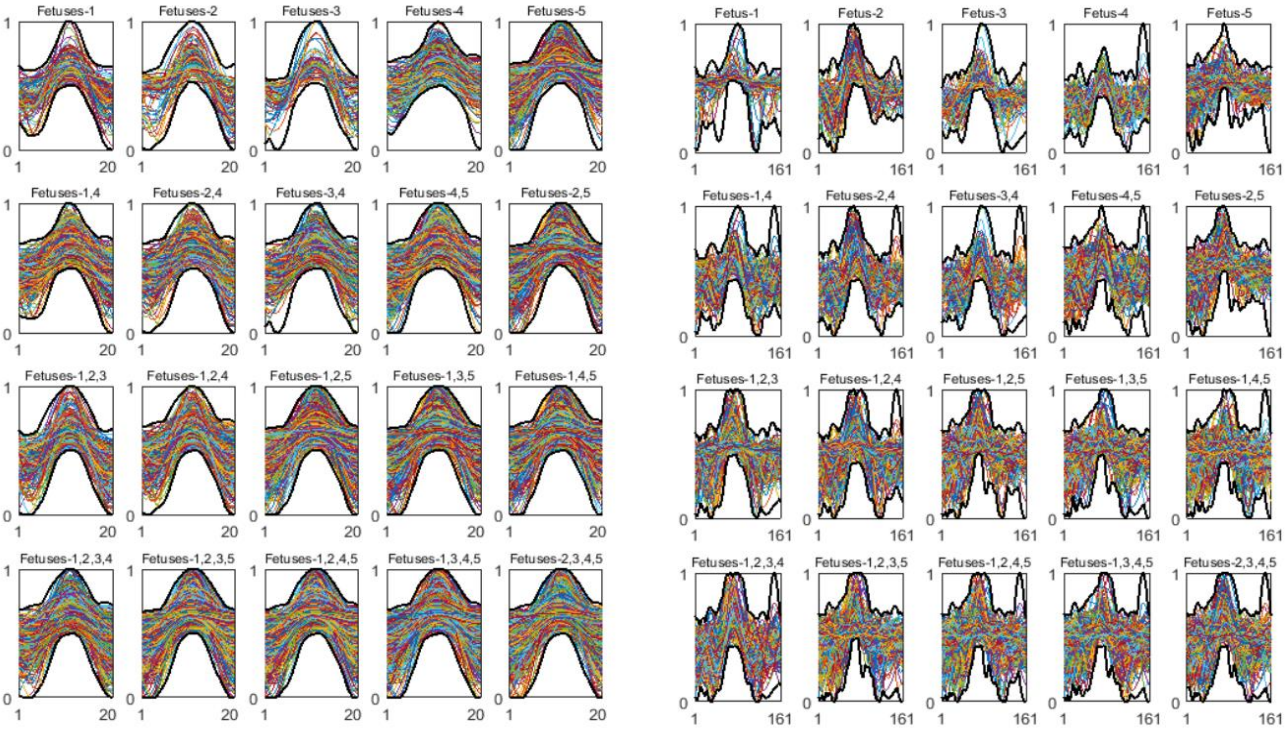

Fig. 9. FOUs obtained from: (A) Daubechies 2, scale 15 at 64Hz (B) Daubechies 2, scale 32 at 1024Hz

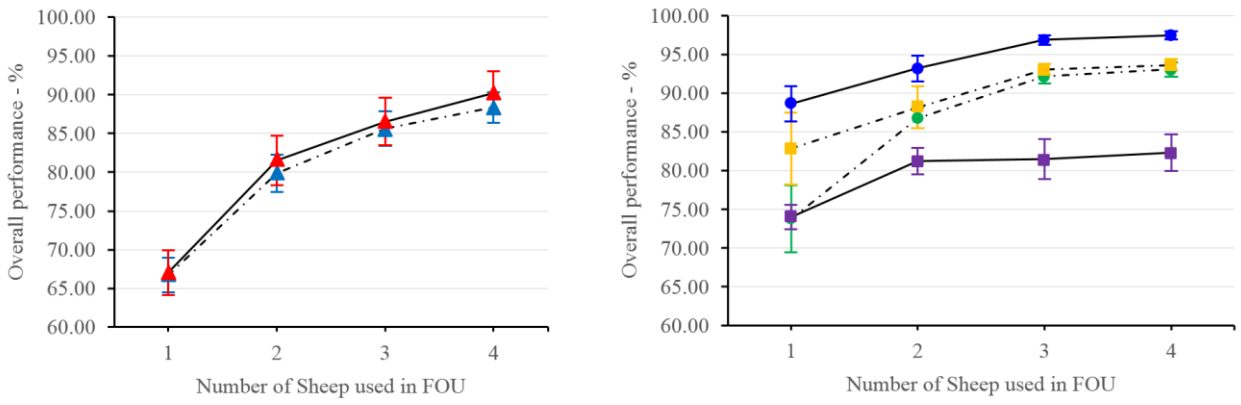

Fig. 10. (A) Bootstrapped overall performance of a Type-2-FLS when FOUs were built from the raw sharp wave profiles for the 64Hz (dotted lines-blue triangles) and 1024Hz (solid lines-red triangles) sampled EEG; (B) Bootstrapped overall performance of the WT-Type-2-FLS classifiers: using Gaussian 2 scale 32 (solid lines-blue circles) at 1024Hz, Daubechies 2 scale 15 (dotted lines-yellow rectangles) at 64Hz, Gaussian 2 of scale 3 (dotted lines-green triangles) at 64Hz and Daubechies 2, scale 32 (dotted lines-purple squares) at 1024Hz.

1024Hz EEG compared to 97%±1 for a Type-2-FLS classifier, where the FOUs were built from Gaussian 2, scale 32, wavelet transformations of the sharp waves from the 1024Hz sampled EEG.

Thus, it is evident that the robust performance of the Type-2-FLS classifier was dependent on building a compact FOUs, strongly supporting our *hypothesis* that a FOU built from a suitable chosen wavelet transformation of the sharp waves provides superior performance over FOUs built from raw sharp waves alone.

The work presented here is concerned specifically on the automatic detection of sharp wave epileptiform transients in the latent phase of the EEG of hypoxic ischemic fetal sheep model [38], which differ in amplitude and duration to sharp waves detected in conventional human EEG [42]. To this end the technique is unique and novel as no other group to date has developed detection methods specifically for this type of sharp wave in this HI animal model as human HI EEG has been concerned primarily with improving the accuracy of seizure detection in the HI EEG of human neonates [31-35, 79, 80].

The only work to date in this area has been our published preliminary results of a more simplified version of the WT-Type-2-FLS method at conference level [38]. This paper presents, for the first time, a WT-Type-2-FLS method to accurately detect sharp wave transients in the EEG recorded after HI and determines a suitable wavelet for both typical clinical 64Hz sampling of the EEG and high, research-based sampling at 1024Hz.

Here we showed that the simplified version of the algorithm [38] which only used certain feature points in the FOU, rather than the whole envelope which we perform in this paper, provided an average overall performance rate of 88% for the detection of sharp waves over the whole latent phase using a Gaussian 2 wavelet. This is in comparison to the 97% obtained here using the whole envelope, thus, providing an improvement of 9% over the simpler method for 1024Hz sampled EEG. The simplified version of the WT-Type-2-FLS method [38] performed even more poorly for the 64Hz sampled EEG providing an average overall performance rate of 37% for the detection of sharp waves over the whole latent phase using a Gaussian 2 wavelet. The performance was dramatically improved upon in the more detailed work presented here obtaining a 94% overall performance using a Daubechies 2 wavelet and the whole envelope as the FOU. Thus, providing an improvement of 57% over the simpler method for 64Hz sampled EEG.

6. Conclusion

In this article, we demonstrate, for the first time, that it is possible to robustly detect sharp wave epileptiform transients accurately in over 30 hours of post-HI EEG for the *in utero* preterm fetal sheep. It was shown that this is possible through initial wavelet transformation of the sharp waves, which serves to stabilize the variation in their profile, and thus permits a highly compact FOU to be built, which in turn optimized the performance of a Type-2 FLS classifier. We demonstrated that this method leads to higher overall performance for both a 64Hz sampled EEG and a high resolution 1024Hz sampled

EEG, compared with both conventional standard wavelet and fuzzy approaches undertaken in isolation.

This study shows that the developed wavelet stabilized FOU method for Type-2-FLS classifiers can be exploited for the identification of epileptiform sharp wave transients during the latent phase of recovery from severe HI in a preterm-equivalent large animal. It should be noted that whilst we have optimized the developed detection method to identify the particular signatures of the sharp wave epileptiform transient in the preterm fetal sheep model, since the approach is generic, it would be possible to adapt the method to detect other forms of epileptiform transient activity and to human models in both children and adults. We believe that this highly automated approach will be valuable for future studies to determine if these micro-scale epileptiform transients are biomarkers of HI.

Acknowledgements

- The work was sponsored by the Health Research Council of New Zealand (HRC grant number 12/613).
- We would also like to acknowledge the contribution of NeSI high-performance computing facilities to the results of this research. URL https://www.nesi.org.nz.

References

1. Back, S. A. (2015). Brain injury in the preterm infant: new horizons for pathogenesis and prevention. *Pediatric neurology*, *53*(3), 185-192.,
2. Drury, P. P., Gunn, E. R., Bennet, L., & Gunn, A. J. (2014). Mechanisms of Hypothermic Neuroprotection. *Clinics in Perinatology*, *41*(1), 161-175.
3. Merchant, N., & Azzopardi, D. (2015). Early predictors of outcome in infants treated with hypothermia for hypoxic–ischaemic encephalopathy. *Developmental Medicine & Child Neurology*, *57*(S3), 8-16.
4. Gunn, A. J., & Bennet, L. (2009). Fetal Hypoxia Insults and Patterns of Brain Injury: Insights from Animal Models. *Clinics in Perinatology*, *36*(3), 579-593.
5. Bennet, L., Roelfsema, V., Pathipati, P., Quaedackers, J. S., & Gunn, A. J. (2006). Relationship between evolving epileptiform activity and delayed loss of mitochondrial activity after asphyxia measured by near-infrared spectroscopy in preterm fetal sheep. *Journal of Physiology*, *572*(1), 141-154.
6. Bennet, L., Booth, L., & Gunn, A. J. (2010). Potential biomarkers for hypoxic-ischemic encephalopathy. *Seminars in Fetal and Neonatal Medicine*, *15*(5), 253-260.
7. Jacobs, S., Berg, M., Hunt, R., Tarnow-Mordi, W., Inder, T., & Davis, P. (2013). Cooling for newborns with hypoxic ischaemic en-cephalopathy. *Status and Date: Edited (no Change to Conclusions), Published In*, (3)
8. Okumura, A., Hayakawa, F., Kato, T., Maruyama, K., Kubota, T., Suzuki, M., Watanabe, K. (2003). Abnormal sharp transients on electroencephalograms in preterm infants with periventricular leukomalacia. *The Journal of Pediatrics*, *143*(1), 26-30.
9. Mandel, R., Martinot, A., Delepoulle, F., Lamblin, M., Laureau, E., Vallee, L., & Leclerc, F. (2002). Prediction of outcome after hypoxic-ischemic encephalopathy: a prospective clinical and electrophysiologic study. *The Journal of Pediatrics*, *141*(1), 45-50.
10. Biagioni, E., Boldrini, A., Bottone, U., Pieri, R., & Cioni, G. (1996). Prognostic value of abnormal EEG transients in preterm and full-term neonates. *Electroencephalography and Clinical Neurophysiology*, *99*(1), 1-9.
11. Walbran, A. C., Unsworth, C. P., Gunn, A. J., & Bennet, L. (2009, September). A semi-automated method for epileptiform transient detection in the EEG of the fetal sheep using time-frequency analysis. In *Engineering in Medicine and Biology Society, 2009. EMBC 2009. Annual International Conference of the IEEE* (pp. 17-20). IEEE.
12. Walbran, A. C., Unsworth, C. P., Gunn, A. J., & Bennet, L. (2011, August). Spike detection in the preterm fetal sheep EEG using Haar wavelet analysis. In *Engineering in Medicine and Biology Society, EMBC, 2011 Annual International Conference of the IEEE* (pp. 7063-7066).
13. Dean, J. M., George, S. A., Wassink, G., Gunn, A. J., & Bennet, L. (2006). Suppression of post-hypoxic-ischemic EEG transients with dizocilpine is associated with partial striatal protection in the preterm fetal sheep. *Neuropharmacology*, *50*(4), 491-503.
14. George, S., Gunn, A. J., Westgate, J. A., Brabyn, C., Guan, J., & Bennet, L. (2004). Fetal heart rate variability and brain stem injury after asphyxia in preterm fetal sheep. *American Journal of Physiology.Regulatory, Integrative and Comparative Physiology*, *287*(4), R925-33.
15. Adeli, H., & Ghosh-Dastidar, S. (2010). Automated EEG-based diagnosis of neurological disorders: Inventing the future of neurology CRC press.
16. Jerger, K. K., Netoff, T. I., Francis, J. T., Sauer, T., Pecora, L., Weinstein, S. L., & Schiff, S. J. (2001). Early seizure detection. *Journal of Clinical Neurophysiology*, *18*(3), 259-268.
17. Faust, Oliver, et al. "Wavelet-based EEG processing for computer-aided seizure detection and epilepsy diagnosis." *Seizure* 26 (2015): 56-64.
18. Adeli, H., Zhou, Z., & Dadmehr, N. (2003). Analysis of EEG records in an epileptic patient using wavelet transform. *Journal of Neuroscience Methods*, *123*(1), 69-87.
19. Rey, H. G., Pedreira, C., & Quiroga, R. Q. (2015). Past, present and future of spike sorting techniques. *Brain Research Bulletin*, *119*, 106-117.
20. Yuan, Q., Zhou, W., Yuan, S., Li, X., Wang, J., & Jia, G. (2014). Epileptic EEG classification based on kernel

sparse representation. *International Journal of Neural Systems, 24*(04), 1450015.
21. Yuan, S., Zhou, W., Yuan, Q., Li, X., Wu, Q., Zhao, X., & Wang, J. (2015). Kernel Collaborative Representation-Based Automatic Seizure Detection in Intracranial EEG. *International Journal of Neural Systems, 25*(02), 1550003.
22. Wilson, S. B., & Emerson, R. (2002). Spike detection: a review and comparison of algorithms. *Clinical Neurophysiology, 113*(12), 1873-1881.
23. Adeli, H., Ghosh-Dastidar, S., & Dadmehr, N. (2007). A wavelet-chaos methodology for analysis of EEGs and EEG subbands to detect seizure and epilepsy. *Biomedical Engineering, IEEE Transactions On, 54*(2), 205-211.
24. Ghosh-Dastidar, S., Adeli, H., & Dadmehr, N. (2007). Mixed-band wavelet-chaos-neural network methodology for epilepsy and epileptic seizure detection. *Ieee Transactions on Biomedical Engineering Bme, 54*(9), 1545.
25. Shah, D. K., Boylan, G. B., & Rennie, J. M. (2012). Monitoring of seizures in the newborn. *Archives of Disease in Childhood.Fetal and Neonatal Edition, 97*(1), F65-9.
26. Sun, H., Juul, H. M., & Jensen, F. E. (2016). Models of hypoxia and ischemia-induced seizures. *Journal of Neuroscience Methods, 260*, 252-260.
27. Cuaycong, M., Engel, M., Weinstein, S. L., Salmon, E., Perlman, J. M., Sunderam, S., & Vannucci, S. J. (2011). A novel approach to the study of hypoxia-ischemia-induced clinical and subclinical seizures in the neonatal rat. *Developmental Neuroscience, 33*(3-4), 241-250.
28. White, A. M., Williams, P. A., Ferraro, D. J., Clark, S., Kadam, S. D., Dudek, F. E., & Staley, K. J. (2006). Efficient unsupervised algorithms for the detection of seizures in continuous EEG recordings from rats after brain injury. *Journal of Neuroscience Methods, 152*(1), 255-266.
29. Abbasi, H., Unsworth, C. P., McKenzie, A. C., Gunn, A. J., & Bennet, L. (2014). Using type-2 fuzzy logic systems for spike detection in the hypoxic ischemic EEG of the preterm fetal sheep. *2014 36th Annual International Conference of the IEEE Engineering in Medicine and Biology Society, EMBC 2014*, 938-941.
30. Abbasi, H., Gunn, A. J., Bennet, L., & Unsworth, C. P. (2015). Reverse Bi-orthogonal wavelets & fuzzy classifiers for the automatic detection of spike waves in the EEG of the hypoxic ischemic pre-term fetal sheep. *Engineering in Medicine and Biology Society (EMBC), 2015 37th Annual International Conference of the IEEE*, 5404-5407.
31. Korotchikova, I., Stevenson, N. J., Walsh, B. H., Murray, D. M., & Boylan, G. B. (2011). Quantitative EEG analysis in neonatal hypoxic ischaemic encephalopathy. *Clinical Neurophysiology, 122*(8), 1671-1678.
32. Temko, A., Thomas, E., Marnane, W., Lightbody, G., & Boylan, G. (2011). EEG-based neonatal seizure detection with Support Vector Machines. *Clinical Neurophysiology, 122*(3), 464-473.
33. Temko, A., Thomas, E., Marnane, W., Lightbody, G., & Boylan, G. B. (2011). Performance assessment for EEG-based neonatal seizure detectors. *Clinical Neurophysiology, 122*(3), 474-482.
34. Temko, A., Stevenson, N., Marnane, W., Boylan, G., & Lightbody, G. (2012). Inclusion of temporal priors for automated neonatal EEG classification. *Journal of Neural Engineering, 9*(4).
35. Temko, A., Boylan, G., Marnane, W., & Lightbody, G. (2013). Robust neonatal EEG seizure detection through adaptive background modeling. *International Journal of Neural Systems, 23*(04), 1350018.
36. Duun-Henriksen, J., Kjaer, T. W., Looney, D., Atkins, M. D., Sørensen, J. A., Rose, M., Juhl, C. B. (2015). EEG Signal Quality of a Subcutaneous Recording System Compared to Standard Surface Electrodes. *Journal of Sensors, 2015*
37. Hansen, G. L., Foli-Andersen, P., Fredheim, S., Juhl, C., Remvig, L. S., Rose, M. H., Johannesen, J. (2016). Hypoglycemia-Associated EEG Changes in Prepubertal Children with Type 1 Diabetes. *Journal of Diabetes Science and Technology*.
38. Abbasi, H., Unsworth, C. P., Gunn, A. J., & Bennet, L. (2014). Superiority of high frequency hypoxic ischemic EEG signals of fetal sheep for sharp wave detection using Wavelet-Type 2 Fuzzy classifiers. *2014 36th Annual International Conference of the IEEE Engineering in Medicine and Biology Society, EMBC 2014*, 1893-1896.
39. Halford, J. J. (2009). Computerized epileptiform transient detection in the scalp electroencephalogram: Obstacles to progress and the example of computerized ECG interpretation. *Clinical Neurophysiology, 120*(11), 1909-1915.
40. McIntosh, G., BAGHURST, K. I., Potter, B., & Hetzel, B. (1979). Foetal brain development in the sheep. *Neuropathology and Applied Neurobiology, 5*(2), 103-114.
41. Buzsáki, G., Anastassiou, C. A., & Koch, C. (2012). The origin of extracellular fields and currents-EEG, ECoG, LFP and spikes. *Nature Reviews Neuroscience, 13*(6), 407-420.
42. International Federation of Societies for Clinical Neurophysiology,. (1974). A glossary of terms most commonly used by clinical electroencephalographers. *Electroencephalography and Clinical Neurophysiology, 37*(5), 538-548.
43. Bennet, L., Dean, J. M., Wassink, G., & Gunn, A. J. (2007). Differential effects of hypothermia on early and late epileptiform events after severe hypoxia in preterm fetal sheep. *Journal of Neurophysiology, 97*(1), 572-578.
44. Keogh, M. J., Drury, P. P., Bennet, L., Davidson, J. O., Mathai, S., Gunn, E. R., Gunn, A. J. (2012). Limited predictive value of early changes in EEG spectral power for neural injury after asphyxia in preterm fetal sheep. *Pediatric Research, 71*(4-1), 345-353.
45. Davidson, J. O., Quaedackers, J. S. L. T., George, S. A., Gunn, A. J., & Bennet, L. (2011). Maternal

dexamethasone and EEG hyperactivity in preterm fetal sheep. *Journal of Physiology, 589*(15), 3823-3835.
46. Mallat, S. G. (2009). A theory for multiresolution signal decomposition: The wavelet representation
47. Mallat, S. (2009). A Wavelet Tour of Signal Processing
48. Unser, M., & Aldroubi, A. (1996). A review of wavelets in biomedical applications. *Proceedings of the IEEE, 84*(4), 626-638.
49. Acharya, U. R., Sree, S. V., Alvin, A. P., Yanti, R., & Suri, J. S. (2012). Application of non-linear and wavelet based features for the automated identification of epileptic EEG signals. *International Journal of Neural Systems, 22*(2), 1250002.
50. Pérez, G., Conci, A., Moreno, A. B., & Hernandez-Tamames, J. A. (2014). Rician noise attenuation in the wavelet packet transformed domain for brain MRI. *Integrated Computer-Aided Engineering, 21*(2), 163-175.
51. Ahmadlou, M., & Adeli, H. (2010). Wavelet-synchronization methodology: a new approach for EEG-based diagnosis of ADHD. *Clinical EEG and Neuroscience, 41*(1), 1-10.
52. Ahmadlou, M., Adeli, H., & Adeli, A. (2011). Fractality and a wavelet-chaos-methodology for EEG-based diagnosis of Alzheimer disease. *Alzheimer Disease and Associated Disorders, 25*(1), 85-92.
53. Adeli, H., Ghosh-Dastidar, S., & Dadmehr, N. (2008). A spatio-temporal wavelet-chaos methodology for EEG-based diagnosis of Alzheimer's disease. *Neuroscience Letters, 444*(2), 190-194.
54. Sankari, Z., Adeli, H., & Adeli, A. (2012). Wavelet coherence model for diagnosis of Alzheimer disease. *Clinical EEG and Neuroscience, 43*(4), 268-278.
55. Ortiz-Rosario, A., Adeli, H., & Buford, J. A. (2015). Wavelet methodology to improve single unit isolation in primary motor cortex cells. *Journal of Neuroscience Methods, 246*, 106-118.
56. Ahmadlou, M., Adeli, H., & Adeli, A. (2010). Fractality and a wavelet-chaos-neural network methodology for EEG-based diagnosis of autistic spectrum disorder. *Journal of Clinical Neurophysiology: Official Publication of the American Electroencephalographic Society, 27*(5), 328-333.
57. Coletta, L. F., Hruschka, E. R., Acharya, A., & Ghosh, J. (2015). Using metaheuristics to optimize the combination of classifier and cluster ensembles. *Integrated Computer-Aided Engineering, 22*(3), 229-242.
58. Ahmadlou, M., & Adeli, H. (2010). Enhanced probabilistic neural network with local decision circles: A robust classifier. *Integrated Computer-Aided Engineering, 17*(3), 197-210.
59. Yu, Y., & McKelvey, T. (2015). A robust subspace classification scheme based on empirical intersection removal and sparse approximation. *Integrated Computer-Aided Engineering, 22*(1), 59-69.
60. Kim, D., Rho, S., Jun, S., & Hwang, E. (2015). Classification and indexing scheme of large-scale image repository for spatio-temporal landmark recognition. *Integrated Computer-Aided Engineering, 22*(2), 201-213.
61. Addison, P. S. (2002). The illustrated wavelet transform handbook: introductory theory and applications in science, engineering, medicine and finance CRC press.
62. Rioul, O., & Vetterli, M. (1991). Wavelets and signal processing. *IEEE Signal Processing Magazine,8*(4),14-38.
63. Lessard, C. S. (2005). Signal processing of random physiological signals. *Synthesis Lectures on Biomedical Engineering, 1*(1), 1-232.
64. Daubechies, I. (1992). *Ten lectures on wavelets* SIAM.
65. Zadeh, L. A. (1965). Fuzzy sets. *Information and Control, 8*(3), 338-353.
66. Karnik, N. N., Mendel, J. M., & Liang, Q. (1999). Type-2 fuzzy logic systems. *IEEE Transactions on Fuzzy Systems, 7*(6), 643-658.
67. Virant-Klun, I., & Virant, J. (1999). Fuzzy logic alternative for analysis in the biomedical sciences. *Computers and Biomedical Research, 32*(4), 305-321.
68. Nauck, D., & Kruse, R. (1999). Obtaining interpretable fuzzy classification rules from medical data. *Artificial Intelligence in Medicine, 16*(2), 149-169.
69. Balasubramanian, K., & Obeid, I. (2011). Fuzzy logic-based spike sorting system. *Journal of Neuroscience Methods, 198*(1), 125-134.
70. Pe, C. A., & Sipper, M. (1999). A fuzzy-genetic approach to breast cancer diagnosis. *Artificial Intelligence in Medicine, 17*(2), 131-155.
71. Güler, I., & Übeyli, E. D. (2005). Adaptive neuro-fuzzy inference system for classification of EEG signals using wavelet coefficients. *Journal of Neuroscience Methods, 148*(2), 113-121.
72. Ahmadlou, M., Adeli, H., & Adeli, A. (2012). Fuzzy synchronization likelihood-wavelet methodology for diagnosis of autism spectrum disorder. *Journal of Neuroscience Methods, 211*(2), 203-209.
73. Ahmadlou, M., & Adeli, H. (2011). Fuzzy synchronization likelihood with application to attention-deficit/hyperactivity disorder. *Clinical EEG and Neuroscience, 42*(1), 6-13.
74. Adeli, H., & Hung, S. (1994). Machine learning: neural networks, genetic algorithms, and fuzzy systems John Wiley & Sons, Inc.
75. Lee, G., Kwon, M., Kavuri, S., & Lee, M. (2014). Action-perception cycle learning for incremental emotion recognition in a movie clip using 3D fuzzy GIST based on visual and EEG signals. *Integrated Computer-Aided Engineering, 21*(3), 295-310.
76. Sugeno, M., & Yasukawa, T. (1993). Fuzzy-logic-based approach to qualitative modeling. *IEEE Transactions on Fuzzy Systems, 1*(1), 7-31.
77. Bachtiar, L. R., Unsworth, C. P., Newcomb, R. D., & Crampin, E. J. (2013). Multilayer perceptron classification of unknown volatile chemicals from the firing rates of insect olfactory sensory neurons and its application to biosensor design. *Neural Computation, 25*(1), 259-287.

78. Bachtiar, L. R., Unsworth, C. P., & Newcomb, R. D. (2014). Using multilayer perceptron computation to discover ideal insect olfactory receptor combinations in the mosquito and fruit fly for an efficient electronic nose. *Neural Computation*,
79. Sherman, D. L., Brambrink, A. M., Walterspacher, D., Dasika, V. K., Ichord, R., & Thakor, N. V. (1997). Detecting EEG bursts after hypoxic-ischemic injury using energy operators. *Engineering in Medicine and Biology Society, 1997. Proceedings of the 19th Annual International Conference of the IEEE, , 3* 1188-1190.
80. Stevenson, N., Korotchikova, I., Temko, A., Lightbody, G., Marnane, W., & Boylan, G. (2013). An automated system for grading EEG abnormality in term neonates with hypoxic-ischaemic encephalopathy. *Annals of Biomedical Engineering, 41*(4), 775-785.